Available online at www.eccomasproceedia.org
Eccomas Proceedia SMART (2023) 1339-1350

ECCOMAS
Proceedia

X ECCOMAS Thematic Conference on Smart Structures and Materials
SMART 2023
D.A. Saravanos, A. Benjeddou, N. Chrysochoidis and T. Theodosiou (Eds)

DESIGN OF A MAGNETORHEOLOGICAL ELASTOMERIC ACTUATOR: ANALYTICAL AND NUMERICAL MODEL WITH EXPERIMENTAL VALIDATION

A. VAIRO*, A. SPAGGIARI†

*Ognibene Power S.p.A.
Via Ing. Enzo Ferrari, 2, 42124 Reggio Emilia RE, Italy
e-mail: antonio.vairo.av@gmail.com, www.ognibene.com

† Department of Sciences and Methods for Engineering (DISMI)
University of Modena and Reggio Emilia
Campus San Lazzaro – Pad Morselli, 42122 Reggio Emilia, Italy
e-mail: andrea.spaggiari@unimore.it, www.dismi.unimore.it

Abstract. This work presents the design and characterization of an innovative linear actuator based on a magneto-rheological elastomer (MRE) coupled to an electromagnet. According to technical literature, this class of materials has many potential applications in engineering fields, ranging from vibration control and suppression to actuator fields and hydraulic applications, such as integrated valves or peristaltic pumps. MREs are a class of smart materials where micrometric magnetic particles are suspended in an elastomeric matrix. We manufactured the MRE by using a 30% volume fraction of carbonyl iron particles in suspension in a commercial RTV silicon matrix, namely Sylgard 184. The MRE was cast in a membrane shape under vacuum, and its magneto-mechanical behaviour was modelled both analytically and by means of finite element simulations. The MRE membrane was coupled with a commercial electromagnet so that the magnetic field was able to provide controlled linear displacement in the axial direction, while the stiffness of the elastomeric matrix was exploited to bring the system back to its initial position. Two membrane thicknesses and two different gaps between the membrane and the electromagnetic actuator were manufactured and tested. Experimental tests were carried out on the actuator by measuring the stroke for a given magnetic field and by applying an external displacement and measuring the force for several current values in the four different actuator configurations. The results confirm that the analytical model can predict the actuator's behaviour in all the various combinations of parameters considered with good precision, which means that it can be easily used as a reliable design tool for this kind of smart system.

Key words: Magnetorheological Elastomers, Design, Actuators, Multiphysics Simulation, Experimental tests.

1 INTRODUCTION

Magnetorheological elastomers (MREs) are a class of smart materials that combine the properties of elastomers and magnetic-rheological (MR) fluids. In recent years, they have gained significant attention due to their unique capability to change their mechanical and

Peer-review under responsibility of the organizing committee of SMART 2023.
doi: 10.7712/150123.9881.449751

rheological properties in response to magnetic fields, making them suitable for use in various applications, including actuators, dampers, and sensors. This article is focused on the use of MREs as actuators and explore their potential as an alternative to conventional actuators. MREs are magnetically controllable materials [1]–[3] with the ferromagnetic particles embedded in an elastomeric solid matrix, rather than suspended in a liquid, giving them some important advantages compared to MR fluids, such as the avoidance of the need for special sealings, and the ability to keep their shape. Applying a magnetic field can also cause a rapid and reversible change in the material's macroscopic mechanical behaviour (elastic and loss modulus). MREs can be controlled as well as MR fluids, as evidenced by various works in technical literature [4], [5], but their application is often limited to research work. Among them many researchers devoted their efforts to describe and model the magneto-mechanical behaviour of MREs, both considering static and dynamic conditions [6]–[11] both through complex analytical models of the viscoelastic rubber matrix and the effect of the magnetic induction field on the global response in terms of storage modulus, loss modulus [10], [12] and failure stress [13].
Potential applications include vibration damping [14], [15], adaptive structures [16], [17], and semi-active systems which take advantage of the change in stiffness of a particular element to modify the vibration response of the structure. Reviews of such applications can be found in the literature.[18]–[20]. Another promising path, though less explored, is the exploitation of MRE capabilities as actuators. Professor Böse and his research group have devoted much effort to this direction, envisioning a potential application of MREs for valve actuation [21]–[24], while Von Lockette exploited MREs as a self-folding mechanism for origami structures [25]. In order to overcome the incapacity of MREs to generate work, de Souza proposed a sandwich system which couples MREs with CFRP skins [26], thus modifying the dynamic response of stiffness. A review of MRE sandwich applications can be found in [27], while a possible application is covered in a patent [28]. One of the most interesting reviews in the MRE actuator field is found in [29], where several examples of variable stiffness devices are reported. Although they can hardly be considered actuators, proper actuators like the soft one proposed by Kashima et al. [30] are retrieved. Generally, it is more difficult to exploit MREs in actuator devices rather than in variable stiffness or shock absorbers devices. Therefore, the aim of this paper is to examine the possible application of MREs as a linear actuator, by exploiting a commercial magnetic circuit coupled with a custom MRE disc. The first section of this work is devoted to the analytical model of the magneto-mechanical system. The second section describes the numerical finite element models that were exploited to validate the design. The actuator manufacturing process and the experimental results show that the proposed idea is feasible and that a simple analytical model may be used as a design tool for these kinds of systems.

2 MATERIALS AND METHODS

2.1 Actuator design and analytical model

This section describes the basic concept underlying the MRE actuator and its main constituents. The idea is to design a linear MRE actuator based on a commercial electromagnet and exploit the MRE to achieve an actuator capable of exerting a certain desired force and/or desired stroke. The schematic in Figure 1a depicts the electromagnetic core in grey, the coil in red as they are provided by the producer [31] This commercial coil (Figure 1b) is capable of providing a force

on its ferromagnetic element up to 1670N with its nominal power 8.2W. The system is powered at 24Vdc with a maximum of 340mA. The turns of the coil are 1750, and the main dimensions are reported in Figure 1a where d_n=35mm, d_e=65mm, h=35mm.
In actuator design the commercial plate is not needed, a ferromagnetic annular spacer, represented in purple in Figure 1, was added and on the top of it, the MRE disc is secured. The ferromagnetic spacer and the MRE are tightened on the electromagnet on the annular periphery, and therefore the system is able to deform as shown in Figure 1b. In order to build an analytical magneto-mechanical model of the system in Figure 1b we simplified the system according to the following hypotheses:

1. We considered a linear B-H curve for the materials, both the MRE and the ferromagnetic core, due to the low field involved and no hysteresis, since the actuation will be low frequency.
2. We considered that all the flux lines stay inside the magnetic yoke and negligible dispersion occurs in the surrounding air.
3. We considered the gap between the magnetic core and the MRE as a constant.

Under these hypotheses it is possible to write the area of the MRE where the flux lines pass as:

$$A_{MRE} = \pi t(R + r) \tag{1}$$

Where *t* is the MRE thickness, *R* the maximum coil diameter and *r* the inner coil diameter in Figure 1a, while the area of the air gap where the electromagnetic field passes is:

$$A_{gap} = \pi\left(r^2 - \frac{d^2}{4}\right) \tag{2}$$

Where *d* is the diameter of the central threaded hole of the electromagnet. Reluctance of the system is mainly given by the sum of reluctance of the air gap $\mathcal{R}_{Gap}$ given by the spacer and the reluctance of the MRE $\mathcal{R}_{MRE}$ which are computed by using eq. (1) and (2).

$$\mathcal{R}_{Tot}(G) = \mathcal{R}_{MRE} + \mathcal{R}_{Gap} = \frac{R - r}{\mu_0 * \mu_{MRE} * A_{MRE}} + \frac{g}{\mu_0 * \mu_{Air} * A_{gap}} \tag{3}$$

Here, μ_0 is the permeability of free space, μ_{MRE} is the relative permeability of the MRE, and μ_{Air} is the permeability of air. To estimate the force exerted by the electromagnet it is useful to exploit the magnetic potential *U*, where *L* is the inductance of the coil, function of the number of turns *N* and the applied current *I*.

$$U = \frac{1}{2}Li^2 = \frac{1}{2}\frac{N^2}{\mathcal{R}_{Tot}}I^2 \tag{4}$$

The magnetic force is obtained through the partial derivative of the potential, recalling eq. (3) as follows:

$$F = \frac{\partial}{\partial G}U = -\frac{N^2 i^2}{2\mu_0\mu_{Air}A_{gap}\mathcal{R}_{Tot}^2} \tag{5}$$

This expression helps in understanding how the magnetic force is influenced by air gap *g* and current *I*, as shown in Figure 2a. The hypothesis under this simple assumption is that the magnetic force acting on the MRE disc, considered in this analytical model, is assumed as a constant, independent on the radial coordinate. This assumption will be assessed using a

numerical simulation in the next section. It is worth noting that the increasing the spacer height (the gap, *g*) decrease the available force but provides room for the linear stroke. The trade-off between force and displacement is normally present in many actuators and can be designed according to the specific needs of the user. This is the motivation that is behind the study of two different air gaps as described in the following sections.

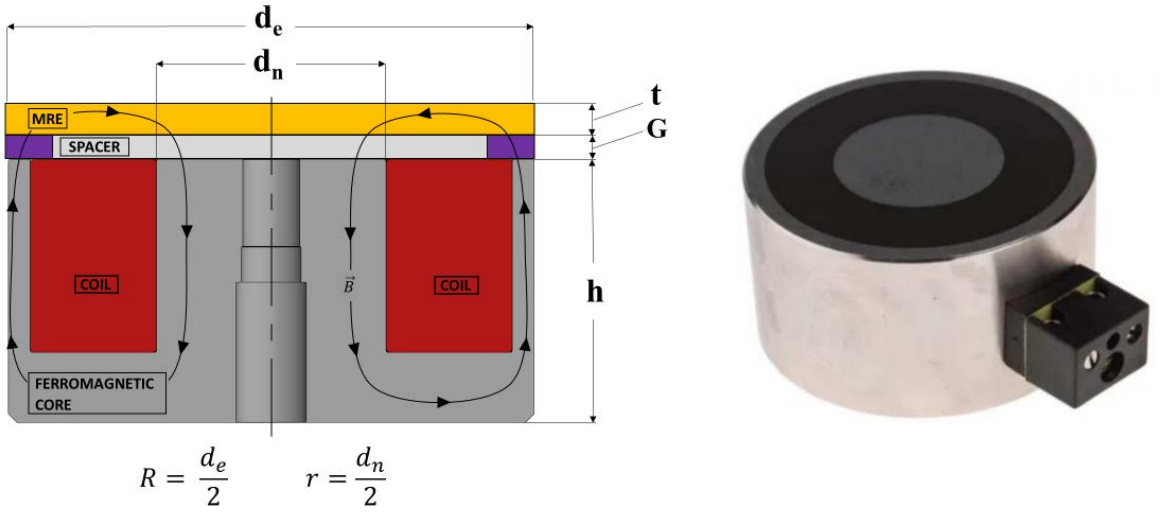

(a) (b)

Figure 1 – Schematic of the actuator (a) and picture of the commercial electromagnet (b)

Now the distributed load q can be calculated as the force over the area of the MRE and, according to [32] the maximum deflection at the center of the MRE disc (Figure 2.b) is easily found as:

$$f = \frac{3qR^4}{16Et^3}(1-\nu^2) \tag{6}$$

Where E and ν are the elastic modulus and the Poisson ration of the MRE respectively.
The two main design variables which can be easily changed and have a strong effect on the actuator properties are therefore g and t and we decided to experimentally test two possibilities for each variable, for a total of four different configurations, as described in Figure 3a. Then the MRE was manufactured as described in [13] with a base elastomer made in Sylgard 184 [33], an RTV silicone already used in many other MRE application [34]–[37] with a 30% in volume of carbonyl iron particles [38]. According to the previous authors work [8] this concentration is optimal to achieve good magneto-mechanical properties such as an elastic modulus of 3 MPa, a Poisson's ratio of 0.49 as for many elastomers and a relative magnetic permeability of , μ_{MRE}=4, which is assumed to be linear in this case. A sample of the MRE disc is reported in Figure 3b, where a very small hole in the center can be noted. This hole is needed to hold the connector where the force will be measured. A central pin will be used in the experiment test to this purpose.

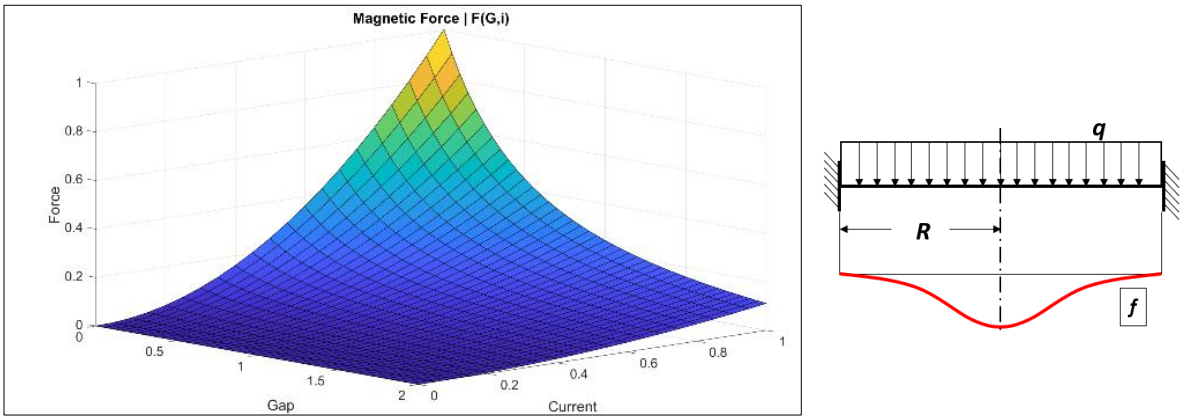

(a) (b)

Figure 2 – Response surface of the magnetic force as a function of the gap and the current (a) and schematic of the MRE disc deflection (b).

	GAP (mm)	MRE thickness (mm)
T4G2	2	4
T4G4	4	4
T6G2	2	6
T6G4	4	6

(a) (b)

Figure 3 – Combination of experimental variables considered in the actuator design and example of MRE discs used in the actuator.

The experimental tests were carried out as follows: first a pulling upward force was applied through the central pin up to 3mm. Then the system is released, and the crosshead of the machine goes down to -1.5mm, the maximum downward stroke. Finally, the system goes back to zero. This cycle, shown in Figure 4a is tested with currents ranging from 0.2 Amps up to 0.8 Amps and with no current to estimate the pure elastic forces, as shown in Figure 4b. The elastic force always opposes to the MRE movement, while the magnetic force always pulls in the downward direction. This peculiarity of the proposed actuator provides an unusual force displacement characteristic. The central hole in the MRE disc is connected to the crosshead with a rigid pin. Although the presence of the central hole and the pin modifies the constraints conditions of the MRE membrane, but it still possible to apply an analytical formula to get the force deflection relationship, as reported in [32].

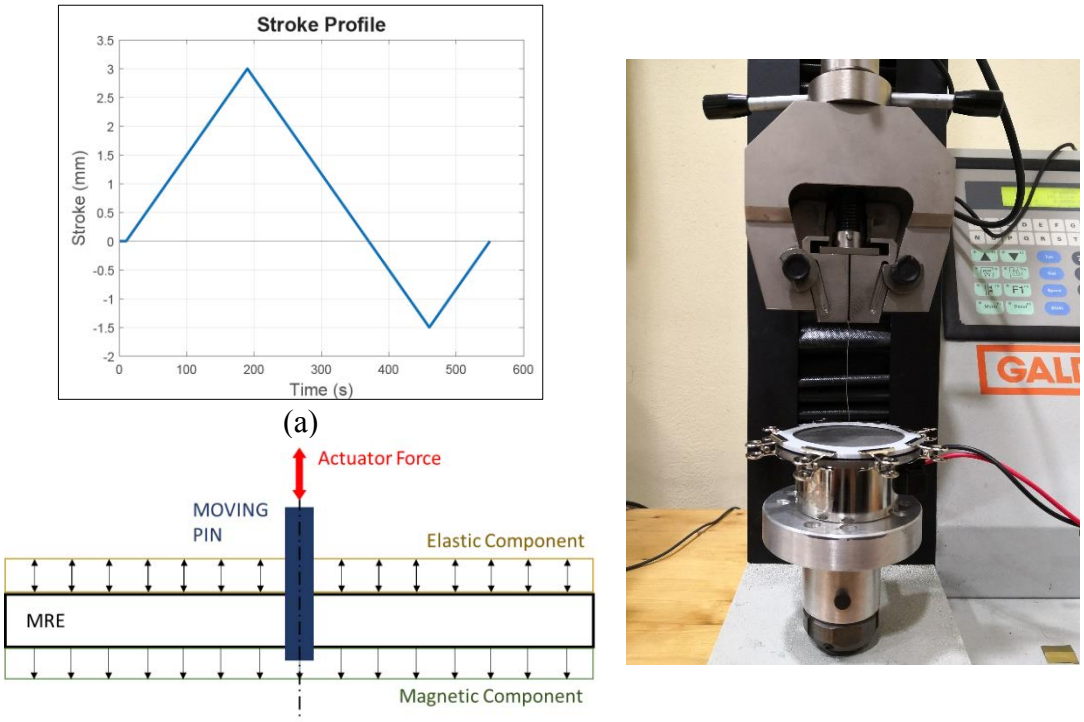

Figure 4 – Experimental stroke profile for the tests (a), forces on the cursor (b) and experimental set up (c)

2.2 Numerical Models

2.2.1 Magnetic FEMM model

The analytical predictions are based on strong assumptions, so a numerical model is needed to verify them. First, we estimated, by means of FEMM software [39], the magnetic induction field which insists on the MRE. The model was created as axially symmetric, and the materials were as reported in the datasheet for the electromagnet, while the MRE is considered linear while the spacer is made of ferritic stainless steel AISI 430 with a relative magnetic permeability of 800. From this model, the analytical prediction in terms of magnetic field inside the MRE and attraction force can be assessed, and the outcome will be presented in the results section. Figure 5a shows the mesh with refinements at the discontinuity in a particular configuration (T6G4), but all four cases were analyzed for increasing current values, ranging from 0.2A up to 0.8A applied for 10 seconds. It is worth noting that the electromagnet datasheet provides a nominal current of 0.340A as the limit for continuous use derived from thermal considerations. In this case, the actuation is quick enough to increase the current to higher levels, thus obtaining a stronger magnetic field and a larger force on the MRE.

2.2.2 Mechanical Finite Element model

The analytical predictions, especially the deflection, are assessed by means of finite element model as shown in Figure 5b. We developed a simple axially symmetric model made using the Simulation tools of Solidworks and imposed the constraints on the periphery of the MRE disc, just like in the physical actuator. The analysis is non-linear and relies on the elastic properties of the MRE mentioned in the previous section. The applied load is obtained from the FEMM analyses described in Section 2.1.1. The output of this model is the deflection at the centre of the MRE disc, which will be compared with the analytical prediction in the Results and Discussion section.

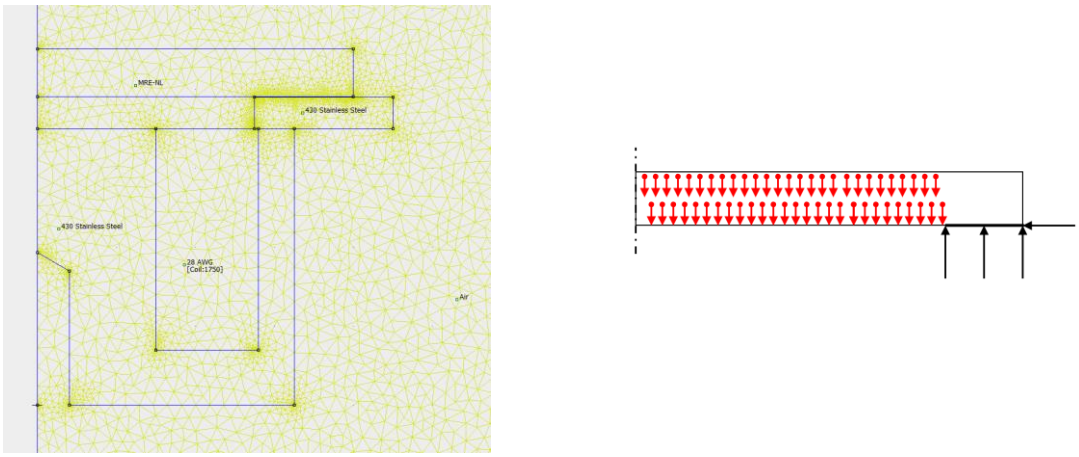

(a) (b)

Figure 5 – FEMM magnetic model (a) and Solidworks simulation model with load taken from (a) and constraints (b)

3 RESULTS AND DISCUSSION

3.1 Numerical Results

3.1.1 Finite element magnetic simulation results

The outcome of the finite element magnetic simulation is reported in Figure 6 for the four configurations considered at a nominal current of 0.5A. The main outcome of this analysis is the force exerted on the MRE element by the electromagnet, which is reported in Table 1. The analysis exploits the axial symmetry of the system, therefore only a half of the model is shown in Figure 6. The computation of the magnetic force, reported in Table 1, already consider the integral over the entire area of the MRE disc.

3.1.2 Finite element mechanical simulation results

The results of the finite element simulations carried out on the MRE membrane as depicted in Figure 7 shows the deformation of the MRE under the forces computed by the FEMM using a linear relationship for the MRE material. Figure 7 represents the axial displacement for the four configurations at the same nominal current of 0.5A.

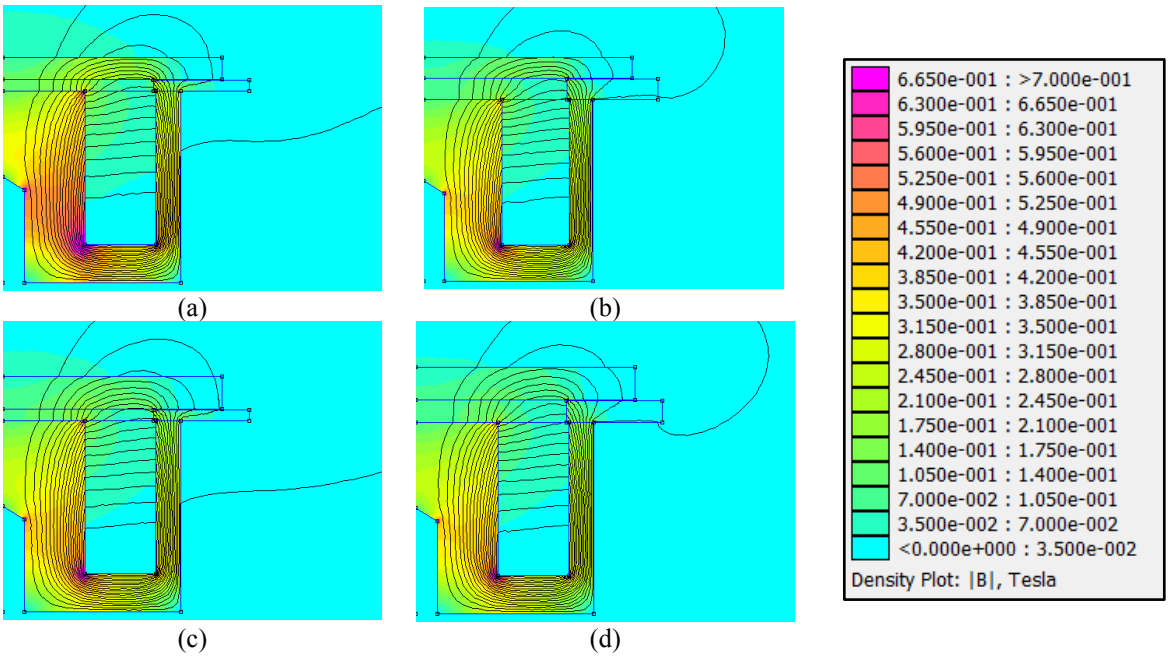

Figure 6 – FEMM simulations at 0.5A for T4G2 (a), T4G4 (b), T6G2 (c) and T6G4 (d).

Table 1 – Numerical magnetic force obtained by simulations (integral on the entire area of the MRE disc).

	Force (N)			
I (A)	**T4G2**	**T4G4**	**T6G2**	**T6G4**
0.1	0,38	0,23	0,48	0,28
0.2	1,53	0,90	1,93	1,10
0.3	3,45	2,05	4,33	2,48
0.4	6,13	3,64	7,70	4,42
0.5	9,58	5,69	12,02	6,90
0.6	13,78	8,19	17,29	9,92
0.7	18,71	11,13	23,46	13,48
0.8	24,35	14,50	30,52	17,56

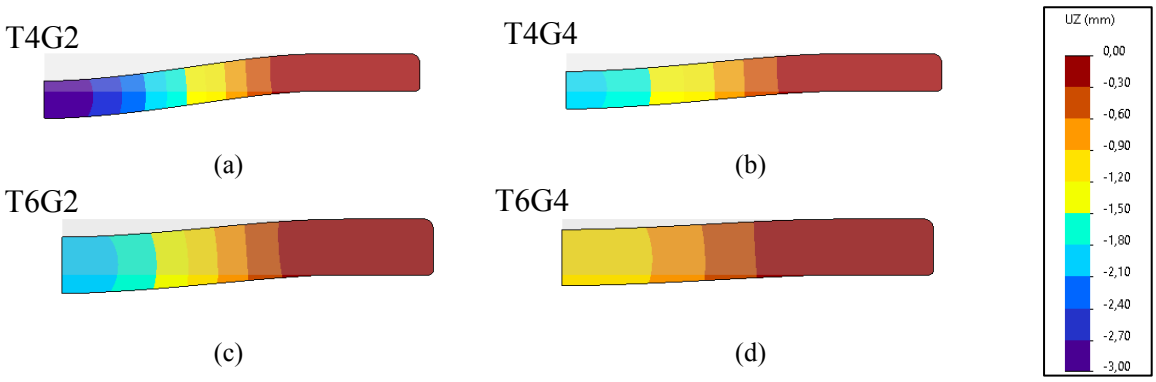

Figure 7 – FEM axial displacement of the MRE disc at 0.5A for T4G2 (a), T4G4 (b), T6G2 (c) and T6G4 (d), superimposed to the unloaded configuration.

3.2 Experimental Results

The experimental tests are reported in Figure 8 for the four combinations of gaps and MRE thicknesses and applied currents. As expected, the force increases with increasing current, and also depending on the stroke, as the MRE disc act as a spring. The force at zero stroke, when the crosshead is blocked, can be interpreted as the net magnetic contribution. When the experimental stroke profile shown in Figure 4a is applied the force first increase, then decreases, and finally returns to its starting values. It should be noted that the stroke is not symmetric, as there are no limitations on the upper stroke allowing the disc to be pulled up to 3mm, while the stroke in lower direction, (shown as negative in Figure 8), is limited by the gap, and fixed at -1.5mm, to prevent the MRE disc from hitting the electromagnet.

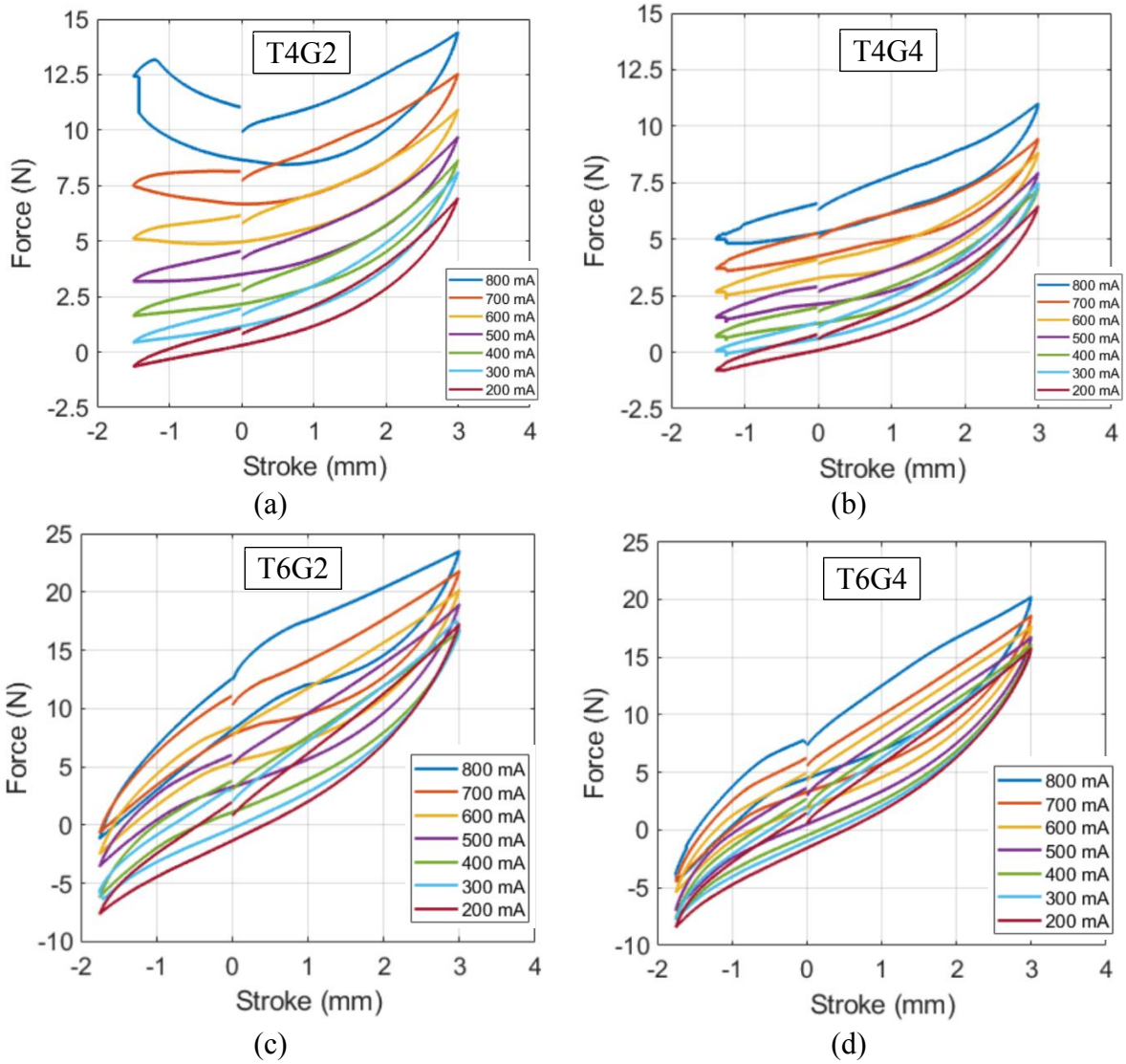

Figure 8 – Experimental Force-displacement curves for the four configurations considered, under the displacement profile applied and for currents ranging from 0.2A to 0.8A. Thickness 4, gap 2 (a), thickness 4, gap 4 (b), thickness 6, gap 2 (c) and thickness 6 gap 4 (d).

By focusing on the forces at zero stroke, it is possible to compare the analytical prediction of the model given by equation (6) and the numerical value obtained by the FEMM simulation. A comparison is provided in Figure 9, where it is immediately clear that the numerical and analytical predictions are in very good agreement, while the experimental ones are always higher in terms of force, especially at high currents. The reason is that the model does not consider the gap reduction due to disc movement and the subsequent increase in the magnetic force. Nonetheless, since the analytical model provides a lower force prediction, it can be safely used for design purposes, and the real application will provide at least the desired force. As it can be seen, the best performance in terms of force is given by a large thickness (6mm) and a low gap (2mm). It is worth noting that lowering the gap has the drawback of lowering the stroke, so a trade-off between the two variables must be found according to the designers' needs.

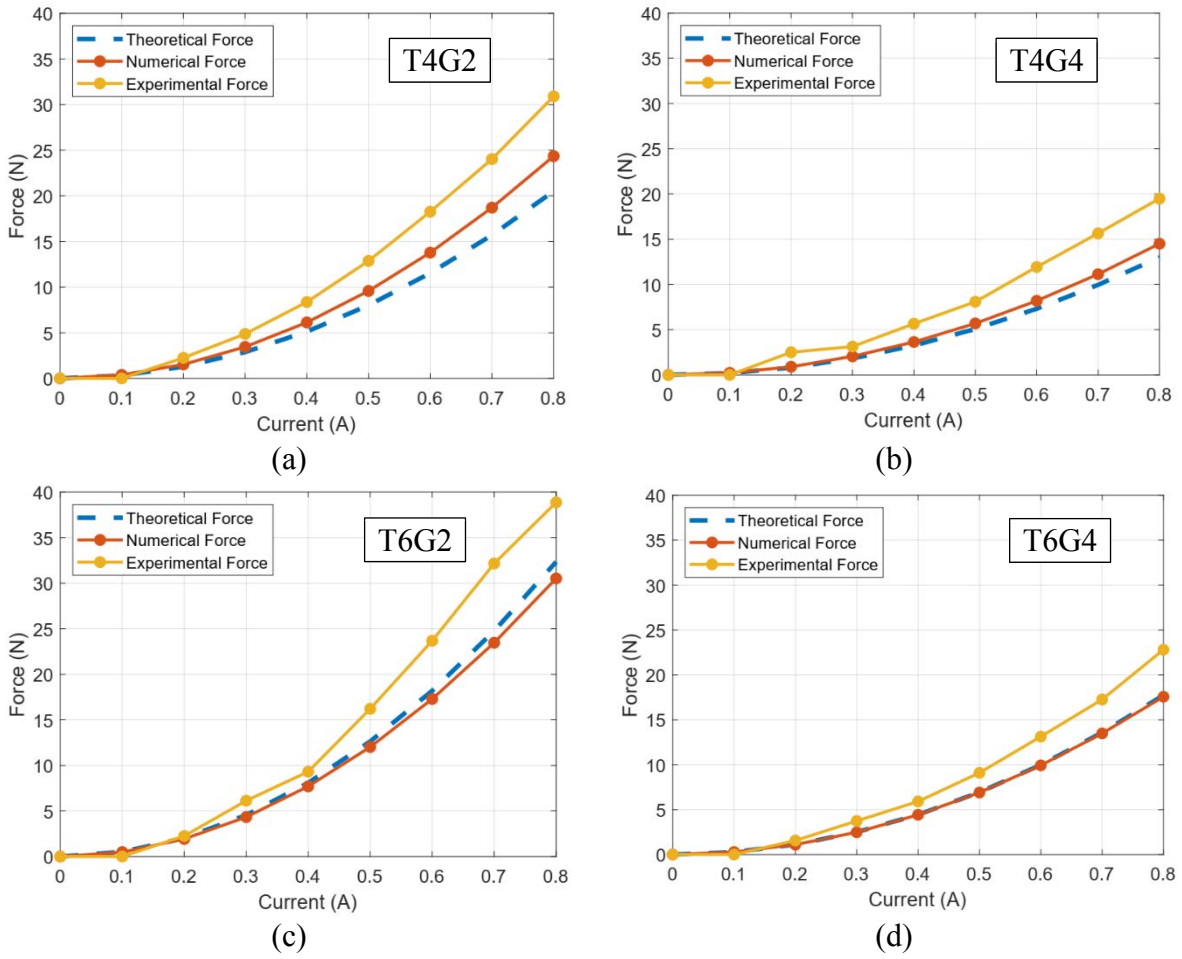

Figure 9 – Comparison between experimental Force at zero displacement for the four configurations considered, for currents ranging from 0.2A to 0.8A. Thickness 4, gap 2 (a), thickness 4, gap 4 (b), thickness 6, gap 2 (c) and thickness 6 gap 4 (d).

4 CONCLUSION

This research study focuses on designing and characterizing an innovative actuator using MRE. The study includes the development of an analytical model to assess the feasibility of the system, mechanical and magnetic finite element simulations to refine the design, and manufacturing and testing of the actuator. The actuator consists of a commercial electromagnet, a MRE disc, and a frame. Four different configurations are analyzed to determine the most suitable arrangement for disc thickness and gap and to verify the accuracy of the analytical and numerical models for design purposes. The study finds that MRE disc thickness, gap, and current significantly affect actuator performance. The experimental results confirm the close agreement between the analytical and numerical models, but both models underestimate the forces exerted by the actuator. The study concludes that the MRE-based linear actuator is feasible, and the analytical model can be applied for design purposes. Future research will focus on improving the model and understanding the influence of the magnetic and elastic components of the actuator's force to enhance the system's controllability.

REFERENCES

[1] M. R. Jolly, J. D. Carlson, and B. C. Muñoz, "A model of the behaviour of magnetorheological materials," *Smart Mater. Struct.*, vol. 5, no. 5, pp. 607–614, Oct. 1996.

[2] M. F. Jaafar, F. Mustapha, and M. Mustapha, "Review of current research progress related to magnetorheological elastomer material," *J. Mater. Res. Technol.*, vol. 15, pp. 5010–5045, Nov. 2021.

[3] H. Böse, T. Gerlach, and J. Ehrlich, "Magnetorheological elastomers — An underestimated class of soft actuator materials," *J. Intell. Mater. Syst. Struct.*, vol. 32, no. 14, pp. 1550–1564, Aug. 2021.

[4] H. Böse and R. Röder, "Magnetorheological elastomers with high variability of their mechanical properties," *J. Phys. Conf. Ser.*, vol. 149, no. 1, p. 012090, Feb. 2009.

[5] A. A. Lerner and K. A. Cunefare, "Performance of MRE-based vibration absorbers," *J. Intell. Mater. Syst. Struct.*, vol. 19, no. 5, pp. 551–563, May 2008.

[6] L. C. Davis, "Model of magnetorheological elastomers," *J. Appl. Phys.*, vol. 85, no. 6, p. 3348, 1999.

[7] Y. Tao, X. Rui, F. Yang, G. Chen, L. Bian, W. Zhu, and M. Wei, "Design and experimental research of a magnetorheological elastomer isolator working in squeeze/elongation–shear mode," *J. Intell. Mater. Syst. Struct.*, vol. 29, no. 7, pp. 1418–1429, Apr. 2018.

[8] A. Bellelli and A. Spaggiari, "Magneto-mechanical characterization of magnetorheological elastomers," *J. Intell. Mater. Syst. Struct.*, vol. 30, no. 17, pp. 2534–2543, 2019.

[9] K. M. Popp, X. Z. Zhang, W. H. Li, and P. B. Kosasih, "MRE properties under shear and squeeze modes and applications," *J. Phys. Conf. Ser.*, vol. 149, p. 012095, Feb. 2009.

[10] M. Kukla, J. Górecki, I. Malujda, K. Talaśka, and P. Tarkowski, "The Determination of Mechanical Properties of Magnetorheological Elastomers (MREs)," *Procedia Eng.*, vol. 177, pp. 324–330, 2017.

[11] G. Schubert and P. Harrison, "Large-strain behaviour of Magneto-Rheological Elastomers tested under uniaxial compression and tension, and pure shear deformations," *Polym. Test.*, vol. 42, pp. 122–134, 2015.

[12] M. Kallio, "The elastic and damping properties of magnetorheological elastomers," VTT Technical Research Centre of Finland, 2005.

[13] A. Spaggiari and A. Bellelli, "Magnetorheological elastomers characterization under shear loading up to failure: A magneto-mechanical multivariate analysis," *J. Intell. Mater. Syst. Struct.*, vol. 32, no. 9, pp. 943–954, May 2021.

[14] A. K. Bastola and L. Li, "A new type of vibration isolator based on magnetorheological elastomer," *Mater. Des.*, vol. 157, pp. 431–436, Nov. 2018.

[15] C. Collette, G. Kroll, G. Saive, V. Guillemier, M. Avraam, and A. Preumont, "Isolation and damping properties of magnetorheologic elastomers," *J. Phys. Conf. Ser.*, vol. 149, p. 012091, Feb. 2009.

[16] Y. L. and J. L. and T. T. and W. Li, "A highly adjustable magnetorheological elastomer base isolator for

applications of real-time adaptive control," *Smart Mater. Struct.*, vol. 22, 2013.
[17] H. Vatandoost, M. Hemmatian, R. Sedaghati, and S. Rakheja, "Dynamic characterization of isotropic and anisotropic magnetorheological elastomers in the oscillatory squeeze mode superimposed on large static pre-strain," *Compos. Part B Eng.*, vol. 182, p. 107648, Feb. 2020.
[18] C. Ruddy, E. Ahearne, and G. Byrne, "A REVIEW OF MAGNETORHEOLOGICAL ELASTOMERS: PROPERTIES AND APPLICATIONS," 2008.
[19] S. Samal, M. Škodová, L. Abate, and I. Blanco, "Magneto-rheological elastomer composites. A review," *Appl. Sci.*, vol. 10, no. 14, Jul. 2020.
[20] A. K. Bastola and M. Hossain, "A review on magneto-mechanical characterizations of magnetorheological elastomers," *Compos. Part B Eng.*, vol. 200, p. 108348, Nov. 2020.
[21] H. Böse, R. Rabindranath, and J. Ehrlich, "Soft magnetorheological elastomers as new actuators for valves," *https://doi.org/10.1177/1045389X11433498*, vol. 23, no. 9, pp. 989–994, Jan. 2012.
[22] M. Cruz, K. U. Kyung, H. Shea, H. Bose, and I. Graz, "Applications of Smart Materials to Haptics," *IEEE Trans. Haptics*, vol. 11, no. 1, pp. 2–4, Jan. 2018.
[23] H. Bose, J. Ehrlich, and T. Gerlach, "Magnetorheological Elastomers-Material Properties and Actuation Capabilities," *IEEE Trans. Magn.*, vol. 58, no. 2, Feb. 2022.
[24] H. Böse, T. Gerlach, and J. Ehrlich, "Magnetorheological elastomers — An underestimated class of soft actuator materials," *J. Intell. Mater. Syst. Struct.*, vol. 32, no. 14, pp. 1550–1564, Aug. 2021.
[25] L. Bowen, K. Springsteen, H. Feldstein, M. Frecker, T. W. Simpson, and P. von Lockette, "Development and validation of a dynamic model of magneto-active elastomer actuation of the origami waterbomb base," *J. Mech. Robot.*, vol. 7, no. 1, Feb. 2015.
[26] F. de Souza Eloy, G. F. Gomes, A. C. Ancelotti, S. S. da Cunha, A. J. F. Bombard, and D. M. Junqueira, "A numerical-experimental dynamic analysis of composite sandwich beam with magnetorheological elastomer honeycomb core," *Compos. Struct.*, vol. 209, pp. 242–257, Feb. 2019.
[27] U. Sharif, B. Sun, S. Hussain, D. S. Ibrahim, O. O. Adewale, S. Ashraf, and F. Bashir, "Dynamic Behavior of Sandwich Structures with Magnetorheological Elastomer: A Review," *Materials (Basel).*, vol. 14, no. 22, Nov. 2021.
[28] Tobias Heier and Christian Schubert, "Actuator having a magnetorheological elastomer element - Google Patents," WO2010054775A1-DE102008057575.5, 2009.
[29] Y. Li, J. Li, W. Li, and H. Du, "A state-of-the-art review on magnetorheological elastomer devices," *Smart Mater. Struct.*, vol. 23, no. 12, Dec. 2014.
[30] S. Kashima, F. Miyasaka, and K. Hirata, "Novel soft actuator using magnetorheological elastomer," *IEEE Trans. Magn.*, vol. 48, no. 4, pp. 1649–1652, 2012.
[31] RS, "Magnetic Door Locks RS PRO TDS." [Online]. Available: https://uk.rs-online.com/. [Accessed: 08-Mar-2023].
[32] W. C. Young and R. G. Budynas, *Roark's Formulas for Stress and Strain, Eighth Edition*. McGraw-Hill Education, 2012.
[33] "Dow Corning Sylgard 184 TDS," 2013. [Online]. Available: https://krayden.com/technical-data-sheet/dow_corning_184_technical_data_sheet/. [Accessed: 13-Sep-2018].
[34] D. Günther, D. Y. Borin, S. Günther, and S. Odenbach, "X-ray micro-tomographic characterization of field-structured magnetorheological elastomers," *Smart Mater. Struct.*, vol. 21, no. 1, 2012.
[35] E. Forster, M. Mayer, R. Rabindranath, H. Böse, G. Schlunck, G. J. Monkman, and M. Shamonin, "Patterning of ultrasoft, agglutinative magnetorheological elastomers," *J. Appl. Polym. Sci.*, vol. 128, no. 4, pp. 2508–2515, May 2013.
[36] W. H. Li and M. Nakano, "Fabrication and characterization of PDMS based magnetorheological elastomers," *Smart Mater. Struct.*, vol. 22, no. 5, p. 055035, Apr. 2013.
[37] A. Bellelli and A. Spaggiari, "Magneto-mechanical characterization of magnetorheological elastomers," *J. Intell. Mater. Syst. Struct.*, vol. 30, no. 17, p. 1045389X1982882, Feb. 2019.
[38] Pometon, "POMETON POWDER," 2017. [Online]. Available: http://www.pometon.com/materialsScheda_eng.php/prodotto=selefer/id_prod=17/from=search. [Accessed: 13-Sep-2018].
[39] D. Meeker, "FEMM 4.2 - Finite Element Method Magnetics Homepage.," 2015. [Online]. Available: http://www.femm.info/Archives/doc/manual42.pdf. [Accessed: 06-Oct-2016].